Two-Phase Densification of Cohesive Granular Aggregates

G. Gioia,[1] A. M. Cuitiño,[2] S. Zheng,[2] and T. Uribe[1]
[1]*Department of Theoretical & Applied Mechanics, University of Illinois, Urbana, Illinois 61801*
[2]*Department of Mechanical & Aerospace Engineering, Rutgers University, Piscataway, New Jersey 08854*
(Received 17 May 2001; published 2 May 2002)

When poured into a container, cohesive granular materials form low-density, open granular aggregates. If pressure is applied to these aggregates, they densify by particle rearrangement. Here we introduce experimental and computational results suggesting that densification by particle rearrangement occurs in the form of a phase transition between two configurational phases of the aggregate. Then we show that the energy landscape associated with particle rearrangement is nonconvex and therefore consistent with our interpretation of the experimental and computational results. Our conclusions are relevant to many technological processes and natural phenomena.

DOI: 10.1103/PhysRevLett.88.204302 PACS numbers: 45.70.Cc

Cohesive granular materials have been the focus of only a small fraction of recent research into the granular state [1]. Yet cohesive granular materials will surely draw increasing attention from scientists and engineers, if only because they are used in numerous applications. One conspicuous application is the forming of ceramic parts, powder metallurgy components, and pharmaceutical tablets by compaction of fine powders [2]. The cohesiveness of powders stems from the large surface-to-volume ratio of their particles, which enhances the effect of attractive van der Waals forces among the particles. In other applications (e.g., the stabilization of soils), the cohesiveness is due to the presence of liquid menisci among the particles. Our interest in the densification of cohesive granular materials was prompted by the recent compaction study of Kong and Lannutti [3]. These authors used x-ray tomography to document the evolution of density during the static compaction of alumina powders (of particle diameter $\sim 60\ \mu$m). By "*static* compaction" we mean that the densification was effected by slowly applying pressure, without shaking. (There exists an important body of work on compaction by shaking, for the most part on noncohesive granular materials [4–6].) Kong and Lannutti reached the tantalizing conclusion that densification "seems to proceed as a wave initiated at the advancing ram" [3]. Our aim here is to elucidate the nature of this 'wave,' and to relate its behavior to the micromechanics of densification in cohesive granular aggregates.

When, preceding compaction, a cohesive granular material is poured into a container, the mobility of the particles reaching the bottom of the container is hindered by the cohesive forces (Fig. 1a). As a result, a low-density, open aggregate of particles is established inside the container (Fig. 1b). Open aggregates densify by particle rearrangement at relatively low pressure [7]. It has been proposed [8] that particle rearrangement occurs when the *rings of particles* of the open aggregate collapse by snap-through buckling (Figs. 1c–1e). To investigate this phenomenon we prepared a quasi-two-dimensional open aggregate [9] by filling a narrow Plexiglas container (of thickness ~ 1.9 mm) with monosized glass beads (of diameter ~ 1.7 mm). Before pouring the beads into the container, we wetted them with water in order for menisci to form among the beads (Fig. 1d). We then compacted the aggregate using a ram. Figure 2a shows three stages during the experiment. A high-density region (composed of the phase H, wherein particle rearrangement has already taken place) and a low-density region (composed of the phase L, wherein the open aggregate remains unchanged) are discernible in the three stages. Densification proceeds by growth of the volume fraction of H at the expense of the volume fraction of L. Visual inspection revealed that no rearrangement occurs within the high- or low-density regions. In a narrow vicinity of the H-L interface or *rearrangement front*, on the other hand, we could observe the collapse by snap-through buckling of successive layers of rings of particles (Fig. 2b). As a result of this process, the rearrangement front (which we identify with the densification wave of Kong and Lannutti) darts forward in the form of broad, very shallow tongues (visible in Fig. 2a). Figure 3 documents two snap-through buckling events taking place during the collapse of a layer of rings of particles.

To gain further insight into the densification of cohesive granular aggregates we conducted a computational simulation. In this simulation, when two particles are pressed together they interact by Hertzian contact. When two particles are pulled away from each other they interact according to a Lennard-Jones potential with a cutoff distance between particles of $d/2$ (where d is the diameter of the particles) and a work of separation of 3.5×10^{-6} Nm (where the work of separation is a measure of the cohesion). The form of interaction between a particle and the container walls (or the ram) is the same as between two particles. We obtained the initial particle aggregate using the ballistic method of Figs. 1a and 1b. We then applied displacement steps to the ram. After each step we allowed the aggregate to relax until the aggregate reached a state of static equilibrium. (This computational relaxation simulates the burst of activity attendant to the application of a

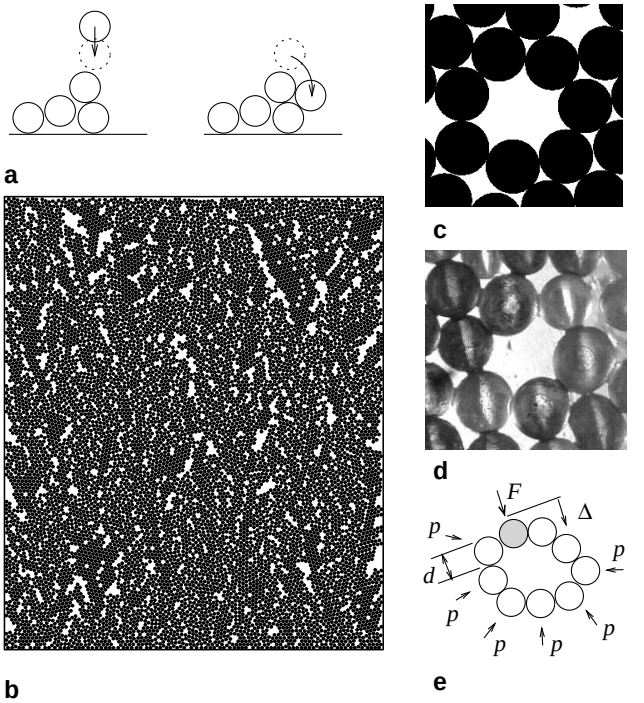

FIG. 1. (a) Computer simulation of container filling by a ballistic aggregation method [14]. The particles are dropped sequentially along random vertical paths, and then allowed to roll down until they make contact with any two points (at least) on the surface of the growing aggregate. The magnitude of the cohesive forces is assumed strong enough to stabilize a particle both at the time of aggregation and afterwards, but it remains otherwise unspecified. (b) Obtained aggregate of particles. (c) More or less regular voids surrounded by rings of particles are a pervasive feature of the simulated aggregate, and also of (d) aggregates obtained in quasi-two-dimensional container-filling experiments. Note the water menisci among the particles. (e) Partial collapse of a ring of particles by snap-through buckling: one of the particles (gray) snaps to the center of the ring. Snap-through buckling events involving more than one snapping particle are possible. After a number of snap-through buckling events have occurred, the void surrounded by the ring disappears. The force F which drives a snap-through buckling event is a relatively large contact force localized on the snapping particle; both photoelastic and numerical studies indicate that such forces exist with magnitudes several times larger than the average contact force [8,15]. The hydrostatic pressure p represents the average contact force [8].

displacement step in the experiment.) Figure 4 shows two stages during the simulation. The high- and low-density regions are visible in both stages, separated by the rearrangement front. As was the case in the experiment (Fig. 2a), densification proceeds by growth of the high-density region at the expense of the low-density region.

Figure 4 also shows plots of the vertical (z-axis) distribution of the aggregate density, $\rho(z)$, plots of the vertical distribution of the root mean square of the vertical displacements of the particles, $u_v(z)$, and plots of the vertical distribution of the root mean square of the horizontal displacements of the particles, $u_h(z)$. [To make these plots we considered a horizontal strip of width w and height h, where w is the width of the container, and $h = 2.5d$. We centered the height of the strip at z, and counted the number $N(z)$ of particle centers contained in the strip. We then computed $\rho(z) = \pi d^2 N(z)/4wh$; $u_v(z) = \sqrt{\Sigma_i (u_v^i)^2}/UN(z)$, where U is the vertical displacement step applied to the ram before reaching the current stage, u_v^i is the vertical displacement of the particle i associated with the step U, and the sum extends over all the particles contained in the strip; $u_h(z) = \sqrt{\Sigma_i (u_h^i)^2}/UN(z)$, where u_h^i is the horizontal displacement of the particle i associated with the step U, and the sum extends over all the particles contained in the strip.] The plots of $\rho(z)$ in Fig. 4 show that at any given stage during the simulation the densities of the high- and low-density regions are spatially uniform, except near the rearrangement front. The plots of $u_v(z)$ show that the high-density region moves vertically together with the ram, whereas the low-density region remains stationary with respect to the container. Finally, the plots of $u_h(z)$ show that as densification proceeds only particles near the rearrangement front move horizontally. These computational results confirm the experimental observation that no rearrangement occurs

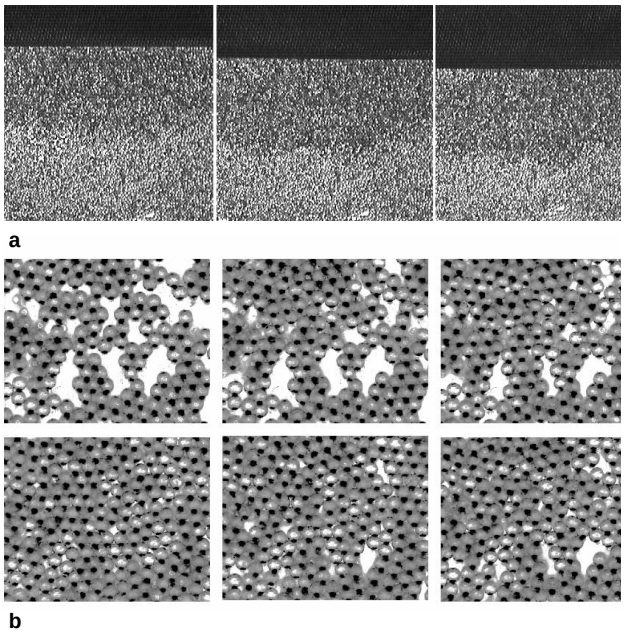

FIG. 2. (a) Three stages during densification. The ram is black, and it advances from the top down in steps of ~2 mm. The high- and low-density regions are dark and light gray, respectively; they are separated by the rearrangement front. The area shown is $\sim 25 \times 25$ cm^2. (b) Clockwise starting from the top left: collapse of successive layers of rings of particles near the rearrangement front. The first photograph in the sequence shows the phase L (the open aggregate). The last photograph in the sequence shows the phase H. The layer of rings of particles closer to the ram collapses first (when reached by the rearrangement front); then, the following layer of rings of particles collapses. Rearrangement occurs only during the advancement of the ram, in a burst of activity; the photographs correspond to states of static equilibrium of the aggregate.

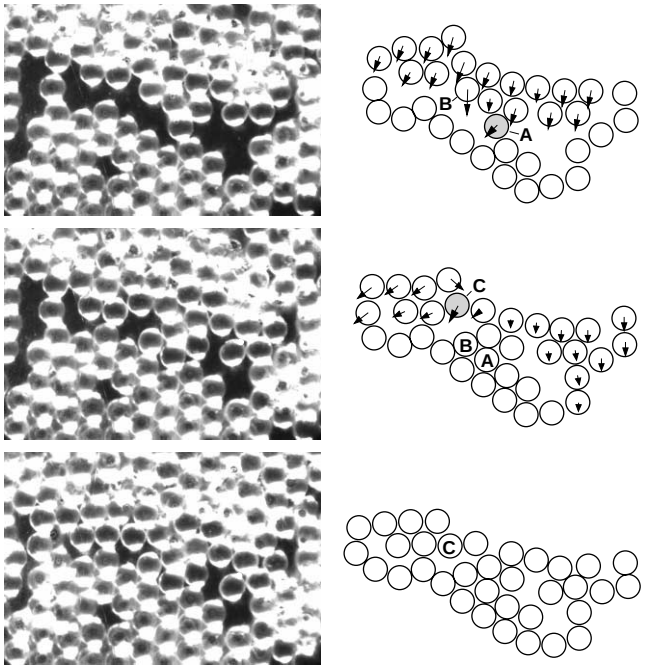

FIG. 3. Three stages during the collapse by snap-through buckling of a layer of rings of particles. From the top down, the stages correspond to increasing displacement of the ram. As in Fig. 2, the ram (not visible here) advances from the top downward in steps of ~2 mm. For each stage the picture on the left is a photograph, and the picture on the right is a diagram obtained from the photograph. The arrows in the first two diagrams are the displacements of the particles when moving from their positions in the current stage to their positions in the following stage. (The absence of an arrow means that the particle does not move.) One snap-through buckling event occurs when the ram advances one step between the first stage and the second; the snapping particle is marked "*A*." Another snap-through buckling event occurs when the ram advances one step between the second stage and the third; the snapping particle is marked "*C*." (Cf. Fig. 1e). As was the case in Fig. 2b, the particles, including those that snap, move only during the advancement of the ram; the photographs correspond to states of static equilibrium of the aggregate.

within the low- or high-density regions (the phases L and H, respectively).

Our experimental and computational investigations suggest that densification occurs in the form of a phase transition $L \rightarrow H$ (Figs. 5a and 5b). To substantiate this statement we start by turning our attention to the micromechanics of particle rearrangement. Consider a ring of particles undergoing snap-through buckling (Fig. 1e). For an increasing displacement Δ (Fig. 5c), the force F vanishes as the particle snaps into the interior of the ring, and again when the particle has entered the ring. Figure 5d shows the attendant evolution of internal energy. The energy associated with the initial (tangent) response of the ring, W_t, is represented by a dashed curve; the relaxation effected by buckling, W_b, is represented by an arrow. The relaxation W_b causes the function $W(\Delta)$ to be nonconvex, i.e., buckling endows the energy landscape with nonconvexity. Nonconvex energy landscapes are characteristic of systems that undergo phase transitions [10].

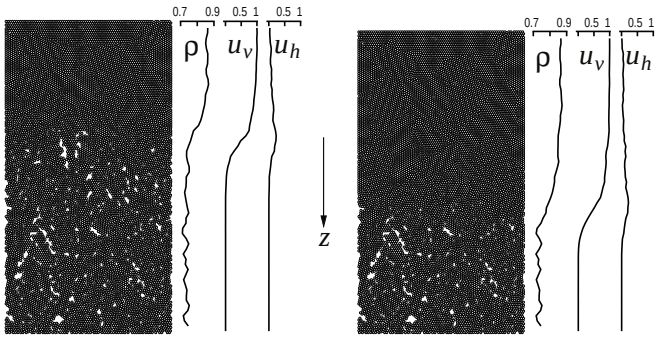

FIG. 4. Two stages during densification in the computational simulation (cf. Fig. 2a). The aggregates are in static equilibrium. ρ is the aggregate density, u_v is the root mean square of the vertical displacements of the particles, and u_h is the root mean square of the horizontal displacements of the particles; we define these quantities in the text.

To move on to the macroscopic scale, we consider an open granular aggregate contained in a *frictionless* container of volume V and constant cross-sectional area. We study the energetics of densification in the space of the local stretch, λ. (The local stretch is defined by $\lambda = \rho_0/\rho$, where ρ is the local density and ρ_0 is the density of the initial open aggregate.) The energy per unit volume is $\phi(\lambda)$ (Fig. 5e); it is nonconvex by inheritance from $W(\Delta)$ (Fig. 5d). The local pressure is given by $p = -d\phi(\lambda)/d\lambda$. We now set the average stretch to

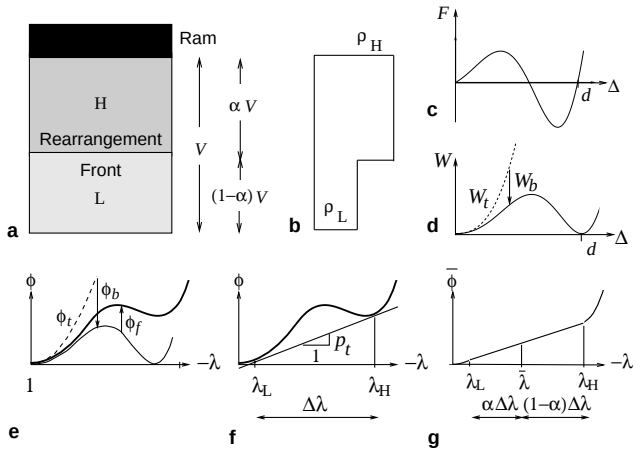

FIG. 5. (a) Interpretation of the experimental results: V is the total volume of the aggregate; the phases H and L are separated by the rearrangement front; α is the volume fraction of H. As α increases from 0 to 1, the rearrangement front sweeps through the aggregate from ram to bottom (cf. Fig. 2a). (b) The density jumps by $\Delta\rho = \rho_H - \rho_L$ across the rearrangement front. (c) Mechanical response of the ring of particles of Fig. 1e: force F vs displacement Δ (schematic); d is the particle diameter. (d) Internal energy W vs Δ. (e) We write the energy per unit volume of the aggregate as $\phi = \phi_t + \phi_b + \phi_f$, where ϕ_t and ϕ_b correspond to the terms W_t and W_b of (d) averaged over a statistically representative volume of aggregate, and ϕ_f is the energy per unit volume dissipated during densification. (f) Geometrical interpretation of the equilibrium equations, [Eq. (1)]. (g) The average energy per unit volume, $\bar{\phi}(\bar{\lambda})$.

a given value, $\bar{\lambda} = 1/V \int_V \lambda \, dV$, and minimize the total energy of the aggregate, $\int_V \phi(\lambda) \, dV$, using conventional tools of nonconvex analysis [10,11]. This leads to the following equilibrium equations:

$$p_t = -\frac{\phi(\lambda_L) - \phi(\lambda_H)}{\lambda_L - \lambda_H} = -\frac{d\phi}{d\lambda}(\lambda_L) = -\frac{d\phi}{d\lambda}(\lambda_H), \quad (1)$$

which allow for the computation of the *characteristic stretches*, λ_L and λ_H, and the *Maxwell pressure*, p_t (Fig. 5f). It is apparent from (1) that λ_L, λ_H, and p_t are independent of $\bar{\lambda}$, and can be construed as properties of the initial open aggregate. The characteristic stretches define two configurational phases, L and H, of density $\rho_L = \rho_0/\lambda_L$ and $\rho_H = \rho_0/\lambda_H$, respectively. When $\lambda_L \geq \bar{\lambda} \geq \lambda_H$, the phase H occupies a volume αV, and the phase L occupies a volume $(1 - \alpha)V$, where $\alpha = (\lambda_L - \bar{\lambda})/(\lambda_L - \lambda_H)$ (Figs. 5a and 5g). As α increases from 0 to 1 during densification, $\bar{\lambda}$ decreases from λ_L to λ_H, the average density increases from ρ_L to ρ_H, and the pressure remains spatially uniform and equal to p_t. We note that $p_t \neq 0$ on account of the dissipation of energy associated with densification (Figs. 5e and 5f). The average energy per unit volume is given by the "convexified" form $\bar{\phi} = \alpha\phi(\lambda_H) + (1 - \alpha)\phi(\lambda_L)$, which for $\lambda_L \geq \bar{\lambda} \geq \lambda_H$ yields the correct value $p = -d\bar{\phi}(\bar{\lambda})/d\bar{\lambda} = p_t$.

We have limited our analysis to the case of a frictionless container. When the container is rough, the pressure is no longer spatially uniform and equal to the pressure applied by the ram; instead, the pressure decreases monotonically away from the ram [12]. It follows that the pressure applied by the ram may reach values much larger than the Maxwell pressure, p_t. Because of the high pressure, both particle rearrangement and particle deformation take place within the high-density region, with a marked effect on the mechanical response of the granular aggregate [13]. We shall further explore these and other effects of wall roughness in a separate publication.

It is instructive to compare our results on static densification by application of pressure with other authors' results on dynamic densification by tapping, i.e., by shaking of the aggregate with pulsed vibrations. The results on dynamic densification by tapping have been obtained by performing Monte Carlo simulations with frustrated lattice-gas models of the granular aggregates [5,6]. In these models, the initial aggregates are open (i.e., low density), even in the absence of cohesive forces; this is so because the particles are assumed to be elongated in shape, and they can therefore be oriented in different ways. The similarities between the dynamic densification predicted by lattice-gas models and the static densification documented in Fig. 2 are revealing. In the Tetris model, for example, the spatial distribution of density is heterogeneous: a high-density region exists in the form of clusters of tightly packed particles. During the dynamic densification of the aggregate, the largest cluster grows at the expense of the smaller ones [6], with the result that the volume fraction of the high-density region grows at the expense of the volume fraction of the low-density region, just as is the case during static densification by application of pressure. The differences are just as revealing as the similarities. For instance, during dynamic densification the overall density of the aggregate increases abruptly, in the form of discrete jumps. In the *persistent times* between successive jumps, the aggregate remains frozen in a state of constant overall density [6]. This irregular, time-dependent evolution indicates that dynamic densification is a temperature-activated phenomenon (and, indeed, the tapping intensity can be construed as an effective temperature of the aggregate [6]). During static densification, on the other hand, particle rearrangement is effected by the pressure; once the pressure reaches the Maxwell pressure, rearrangement takes place without delay, simultaneously with the advancement of the ram.

This work has been supported by a grant from the International Fine Particle Research Institute. G. G. acknowledges partial support from the UIUC Research Board and from a UIUC Critical Research Initiative.

[1] H. M. Jaeger and S. R. Nagel, Science **255**, 1523 (1992).
[2] K. G. Ewsuck, MRS Bull. **22**, 14 (1997).
[3] C. M. Kong and J. J. Lannutti, J. Am. Ceram. Soc. **83**, 685 (2000).
[4] S. E. Edwards and R. B. S. Oakeshott, Physica (Amsterdam) **157A**, 1081 (1989); H. M. Jaegger, S. R. Nagel, and R. P. Behringer, Rev. Mod. Phys. **68**, 1259 (1996).
[5] M. Nicodemi, A. Coniglio, and H. J. Hermann, J. Phys. A **30**, L379 (1997); *Physics of Dry Granular Media*, edited by H. J. Hermann *et al.* (Kluwer, Dordrecht, 1998); J. J. Arenzon, J. Phys. A **32**, L107 (1999); M. Nicodemi and A. Coniglio, Phys. Rev. Lett. **82**, 916 (1999); M. Nicodemi, Phys. Rev. Lett. **82**, 3734 (1999).
[6] M. Nicodemi, Physica (Amsterdam) **285A**, 267 (2000).
[7] D. E. Niesz, R. B. Bennett, and M. J. Snyder, Ceram. Bull. **51**, 677 (1972).
[8] L. T. Kuhn, R. M. McMeeking, and F. F. Lange, J. Am. Ceram. Soc. **74**, 682 (1991).
[9] H. M. Jaeger, J. B. Knight, C. Liu, and S. R. Nagel, MRS Bull. **19**, 25 (1994).
[10] J. L. Ericksen, *Introduction to The Thermodynamics of Solids* (Springer-Verlag, New York, 1998), 2nd ed., Chap. 3.
[11] G. Gioia, Y. Wang, and A. M. Cuitiño, Proc. R. Soc. London A **457**, 1079 (2001).
[12] B. J. Briscoe and P. D. Evans, Powder Technol. **65**, 7 (1991).
[13] G. Gioia and A. M. Cuitiño, (to be published).
[14] R. Jullien and P. Meakin, Europhys. Lett. **4**, 1385 (1987).
[15] C.-H. Liu, S. R. Nagel, D. A. Schecter, S. N. Coppersmith, S. Majumdar, O. Narayan, and T. A. Witten, Science **269**, 513 (1995); S. N. Coppersmith, Physica (Amsterdam) **107D**, 183 (1997).